Invertebrate Biology 125(1): 21–33.

DOI: 10.1111/j.1744-7410.2006.00036.x

Embryonic development and shell differentiation in *Chione cancellata* (Bivalvia, Veneridae): an ultrastructural analysis

Marcel Mouëza, Olivier Gros,[a] and Liliane Frenkiel

Département de Biologie, Laboratoire de Biologie Marine, Université des Antilles et de la Guyane, 97159 Pointe-à-Pitre Cedex, Guadeloupe, France

Abstract. The embryonic development in *Chione cancellata,* from fertilization to straight-hinge D-stage veliger larva, occurs in 24 h at 25°C. Transmission (TEM) and scanning (SEM) electron microscopy show that morphogenetic processes result in a gastrula with two depressions, 4 h after fertilization (T_0+4 h). Two hours later, one depression, located at the animal pole, develops into an open cave, the floor of which becomes the shell field, characterized by scarce microvilli, located below the lower face of the prototrochal pad. The invagination located at the vegetal pole is characterized by regular microvilli and constitutes the digestive tract. At T_0+8 h, the late gastrula differentiates into a typical motile trochophore, possessing a well-developed prototroch delimiting anterior and posterior embryonic regions. At T_0+9 h, the shell field, located between the prototroch and the telotroch, appears as a saddle-shaped region with a wrinkled surface extending on both sides of the embryo, establishing bilateral symmetry. From TEM observations, the apical surface of the underlying cells possesses a modified glycocalyx featuring a dense pellicle overlapping the cells of the shell field. At T_0+12 h, the prototroch is displaced toward the anterior region by outgrowth of the shell material. TEM views show that the wrinkled surface observed with SEM corresponds to the periostracum, attached dorsally to the hinge and ventrally to the cells of the future mantle edge. At T_0+15 h, an alveolar matrix of proteinaceous material, which could contain calcite crystals, appears between the periostracum and the mantle. At T_0+24 h, prodissoconch I formation is completed and the D-stage larvae possess a calcified shell. At this stage of development, only one mantle fold is present, representing the outer fold. The periostracum-secreting cells are in contact with the marginal cells of the velum. This functional velum is composed of four bands of cilia. Our TEM observations confirm previous descriptions of the velum ciliary bands obtained only from SEM analyses, such as described in other bivalves. The apical sense organ and the digestive tract are poorly developed. From observations at the ultrastructural level of shell differentiation in *C. cancellata,* we propose a new interpretation of shell differentiation, including hinge and ligament for bivalves as opposed to that described for gastropods.

Additional key words: mollusca, bivalvia, ontogenesis, shell differentiation

In Eulamellibranchia, larval development has been described in a number of species with as much detail as possible using light microscopy (Loosanoff & Davis 1963; Loosanoff et al. 1966; Frenkiel & Mouëza 1979; Sastry 1979). This includes some developmental stages of venerid species (for review, see Mouëza et al. 1999) such as *Chione stutchburyi* Gray 1828 (Stephenson & Chanley 1979) and *Chione cancellata* Linné 1787 (D'Asaro 1967; LaBarbera & Chanley 1970). The first observation of the embryonic development of the shell-field invagination was described in gastropods by Gegenbaur and in bivalves by Stepanoff a century ago (in Kniprath 1980). These observations were limited to light microscopy; Humphreys (1969), followed by Kniprath (1980), initiated a study of the early shell-field formation in *Mytilus edulis* Linné 1758 with transmission electron microscopy (TEM).

Developmental studies using electron microscopy are still scarce and generally deal with specific

[a] Author for correspondence.
E-mail: olivier.gros@univ-ag.fr

features like hinge structure (Stephenson & Chanley 1979) or shell morphogenesis (Carriker & Palmer 1979; Hodgson & Burke 1988) observed in scanning electron microscopy (SEM) during larval development. More recently, some papers were published about the embryonic development of bivalves with SEM analysis, such as those on scallops (Hodgson & Burke 1988; Bellolio et al. 1993), lucinids (Gros et al. 1997, 1999), on a venerid (Mouëza et al. 1999), and on a nuculid (Zardus & Morse 1998). A few papers have combined TEM and SEM analysis as those of Eyster & Morse (1984) on *Spisula solidissima* Dillwyn 1817, Casse et al. (1998) on *Pecten maximus* Linné 1758, and Zardus & Morse (1998) on *Acila castrensis* Hinds 1843. Eyster & Morse (1984) pointed out that many histological sections, in any given embryo, may give the erroneous impression that the shell-field invagination is closed and that many questions about very early shell formation remain unanswered. A comparative study using SEM and TEM at key stages of various species may help to clarify the shell formation processes in bivalves.

Chione cancellata is a tropical venerid bivalve distributed from North Carolina to Brazil (Warmke & Abbott 1962; Abbott 1974; Rios 1985). It lives at 0.5–1.5 m water depth, shallowly burrowed in the muddy sand of mangrove lagoons. The embryonic development in *C. cancellata,* from fertilization to the straight-hinge veliger D-stage larva, occurs within 24 h at 25°C, which allows a good coverage of embryonic stages by regular, 1-h intervals of fixation over this time lapse.

The purpose of the present article is to compare patterns of development in tropical venerids and investigate selected aspects of ontogenesis to introduce a new interpretation of shell differentiation in bivalves.

Methods

Fertilization and embryonic rearing

Adults of *Chione cancellata* were collected by hand in shallow water in mangrove lagoons off the island of Guadeloupe in the French West Indies. For each spawning trial, a dozen freshly collected venerids were cleaned and kept dry for 1–2 h. Then, individuals were placed in a 50-L tank filled with seawater until the onset of spawning. Each spawning female was quickly transferred to a new 50-L tank, so as to sequester unfertilized oocytes in the new tank. Following this, sperm from several males was pooled and added to the tank with oocytes 30 min after onset of spawning to obtain synchronous fertilization. Development proceeded at room temperature, i.e., 25°C, in seawater at a salinity of 35–37‰, which is typical for their natural habitat. No antibiotics were used and all seawater used for fertilization and rearing was filtered through a 5-μm Millipore cartridge filter and then UV treated (Proteco LM6-S86, Proteco, Pamproux, France: 2×80 W). The rearing tanks were gently aerated with 0.22-μm-filtered air bubbling in order to avoid sedimentation of eggs and embryos during the embryonic period.

Electron microscopy

Every hour throughout embryonic development, 2 L of seawater containing several thousand embryos were collected on a 26-μm-mesh nylon screen. The embryos were quickly placed in small baskets for safe handling during the fixation. At each time point, two samples were obtained, one for SEM observation and the other for TEM.

Scanning electron microscopy

Embryos were fixed at 4°C for 1 h in 2.5% glutaraldehyde in 0.1 mol L^{-1} cacodylate buffer, adjusted to pH 7.2 and 900 mOsm with 0.4 mol L^{-1} NaCl and 2 mmol L^{-1} $CaCl_2$. After a rinse in the same cacodylate buffer, embryos were dehydrated in an ascending series of acetone dilutions and critical point dried using CO_2 as transitional fluid. Embryos were then sputter coated with gold before observation in a SEM Hitachi S-2500 (Elexience, Verrières-le-Buisson, France) at 20 kV.

Transmission electron microscopy

Embryos were prefixed for 1 h at 4°C following the same procedure as for SEM. They were then fixed for 45 min at room temperature in 1% osmium tetroxide in the same buffer, rinsed in distilled water, and postfixed with 2% aqueous uranyl acetate for 1 h. No decalcification process was undertaken. After a rinse in distilled water, each sample was dehydrated through a graded ethanol series and embedded in Epon-araldite according to Mollenhauer (in Glauert 1975). Sections were cut using an UltracutE Leica ultramicrotome (Leica, Reuil-Malmaison, France); thin sections (70 nm thick) were collected on coated 100-mesh grids, contrasted 30 min in 2% aqueous uranyl acetate and 10 min in 0.1% lead citrate before examination in a TEM (Hitachi H-8000) at 100 kV.

Results

Adults of *Chione cancellata* spawned in the laboratory throughout the year by keeping them dry for

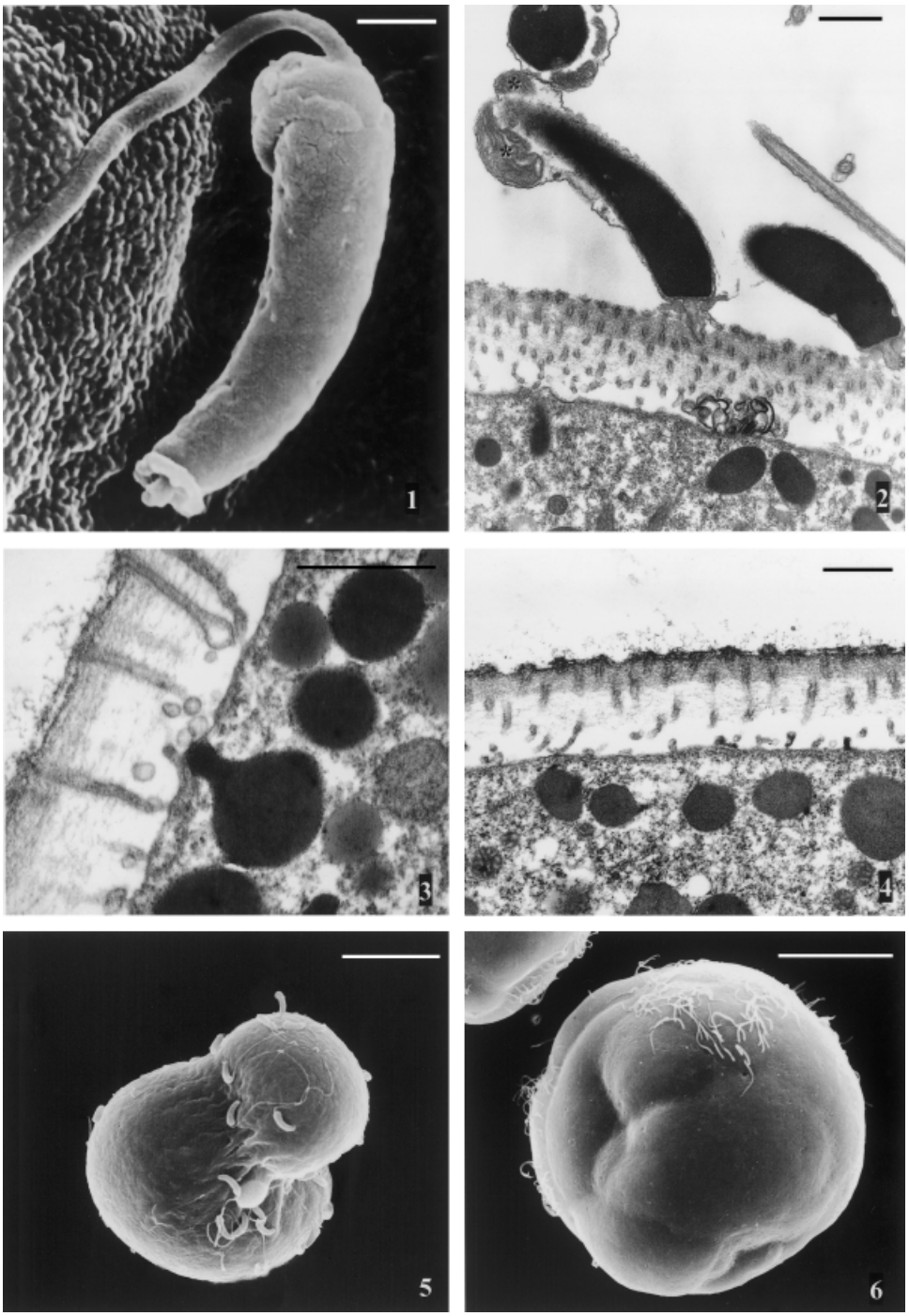

Figs. 1–6. Gametes, eggs, and young embryos of *Chione cancellata*. **Fig. 1.** Sperm lying on the surface of an oocyte. It is characterized by a short arched head with an elongated acrosome protected by a thick envelope that has broken down. Scanning electron microscopy (SEM). Scale bar, 0.3 μm. **Fig. 2**. Initial fertilization wherein the inner membrane of the acrosome is linked to the ovular microvilli. Two mitochondria from the mid-piece can be observed (asterisks). Transmission electron microscopy (TEM). Scale bar, 1 μm. **Fig. 3.** After fertilization, a thickening of the glycocalyx, the vitelline envelope, forms because of the extrusion of dense material from numerous cytoplasmic globules. TEM. Scale bar, 0.5 μm. **Fig. 4.** A fertilization membrane-like structure appears quickly after fertilization because of the material expelled from the cytoplasmic vesicles underlying the cell membrane. This material builds up a dense layer at the tip of microvilli. TEM. Scale bar, 0.5 μm. **Fig. 5.** Two-cell embryo with unequal blastomeres. A polar body is located in the cleavage furrow and spermatozoa are scattered on the surface of the embryo. SEM. Scale bar, 10 μm. **Fig. 6.** Early gastrula, T_0+4 h. There are two weak depressions in the vegetal pole. The first cilia of the future prototroch are differentiated in the anterior region. SEM. Scale bar, 10 μm.

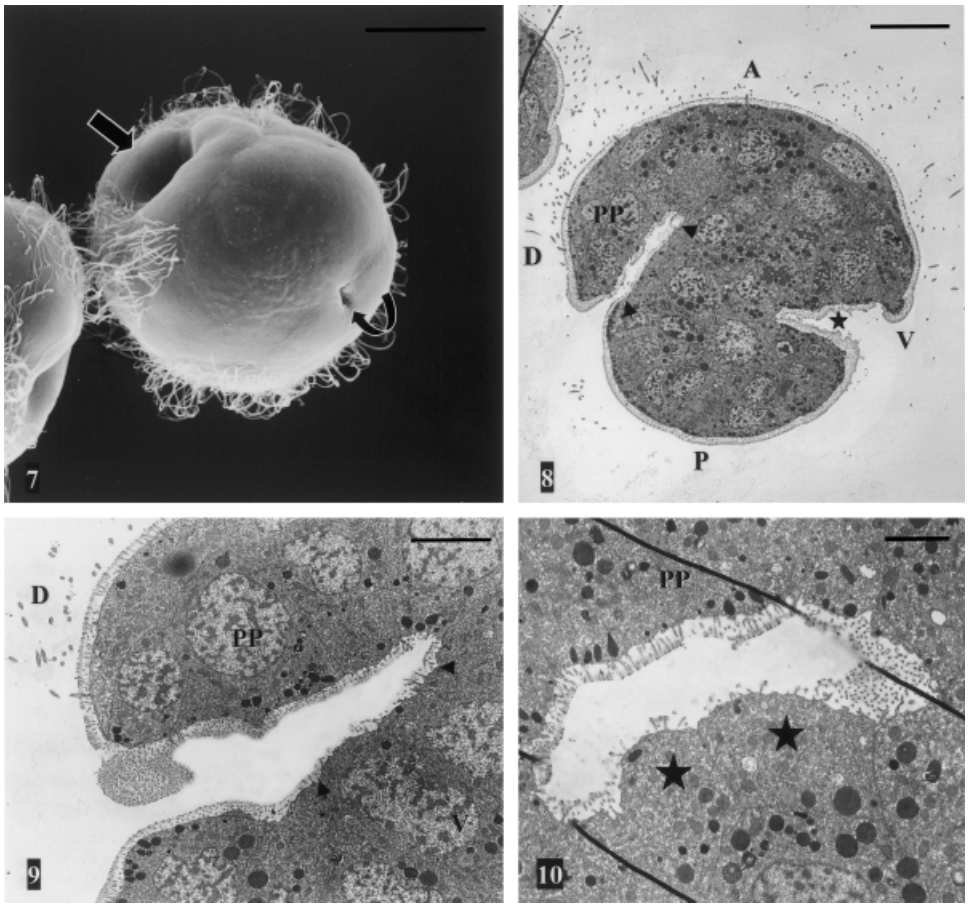

Figs. 7–10. Shell-field differentiation in gastrulae of *Chione cancellata* at T_0+6 h. **Fig. 7.** The gastrula is characterized by two depressions: a small round blastopore anteriorly (curved arrow) and a large open cave posteriorly (straight arrow). Scanning electron microscopy (SEM). Scale bar, 10 μm. **Fig. 8.** Sagittal section of a gastrula. The dorso-ventral axis (DV) extends from the prototrochal pad (PP) through the shell field (delineated by arrowheads) up to the blastopore. The microvilli constitute a thick brush border in the archenteron (star), whereas they are scarce in the shell field. AP, antero-posterior axis. Transmission electron microscopy (TEM). Scale bar, 10 μm. **Fig. 9.** Higher magnification of the sagittal section along the dorso-ventral axis (DV). The section extends through the prototrochal pad, the lumen of the open cave, and the shell field. The prototrochal pad (PP) overlies the shell field (delineated by arrowheads). TEM. Scale bar, 5 μm. **Fig. 10.** Cross-section through the pad of the prototroch (PP) and shell field cells (stars). The shell field comprises a few cells in which microvilli progressively regress. These cells will elaborate the periostracum. TEM. Scale bar, 0.5 μm.

periods of 1–2 h before placing them back in seawater. Oocytes, 60 μm in diameter, do not have a prominent jelly coat and usually possess a prominent germinal vesicle. No polar lobe was observed. Sperm appear very active, and are characterized by a short arched head, 1 μm long, and a 50-μm-long flagellum (Fig. 1). The acrosome is elongated and protected by a thick outer envelope which breaks down on contact with the ovular microvilli and glycocalyx (Figs. 1, 2). Polyspermy may occur but does not affect embryonic development. After fertilization, the glycocalyx thickens because of the extrusion of a dense material from numerous cytoplasmic globules. It appears to constitute the vitelline envelope (Fig. 3). The superficial layer of the glycocalyx becomes denser and constitutes a fertilization membrane-like structure (Fig. 4).

The first polar body appears ~10 min after contact between oocytes and sperm (T_0+10 min). The first cleavage occurs 30 min after fertilization and results in two unequal blastomeres, AB and CD, without a polar lobe. The polar bodies are located in the cleavage furrow (Fig. 5). Successive cleavages produce an intermediate morula, which develops quickly into a blastula with a few cilia on its surface. It is the first mobile stage in the embryonic development. The early gastrula (Fig. 6) differentiates 4 h after fertilization (T_0+4 h). Morphogenetic movements

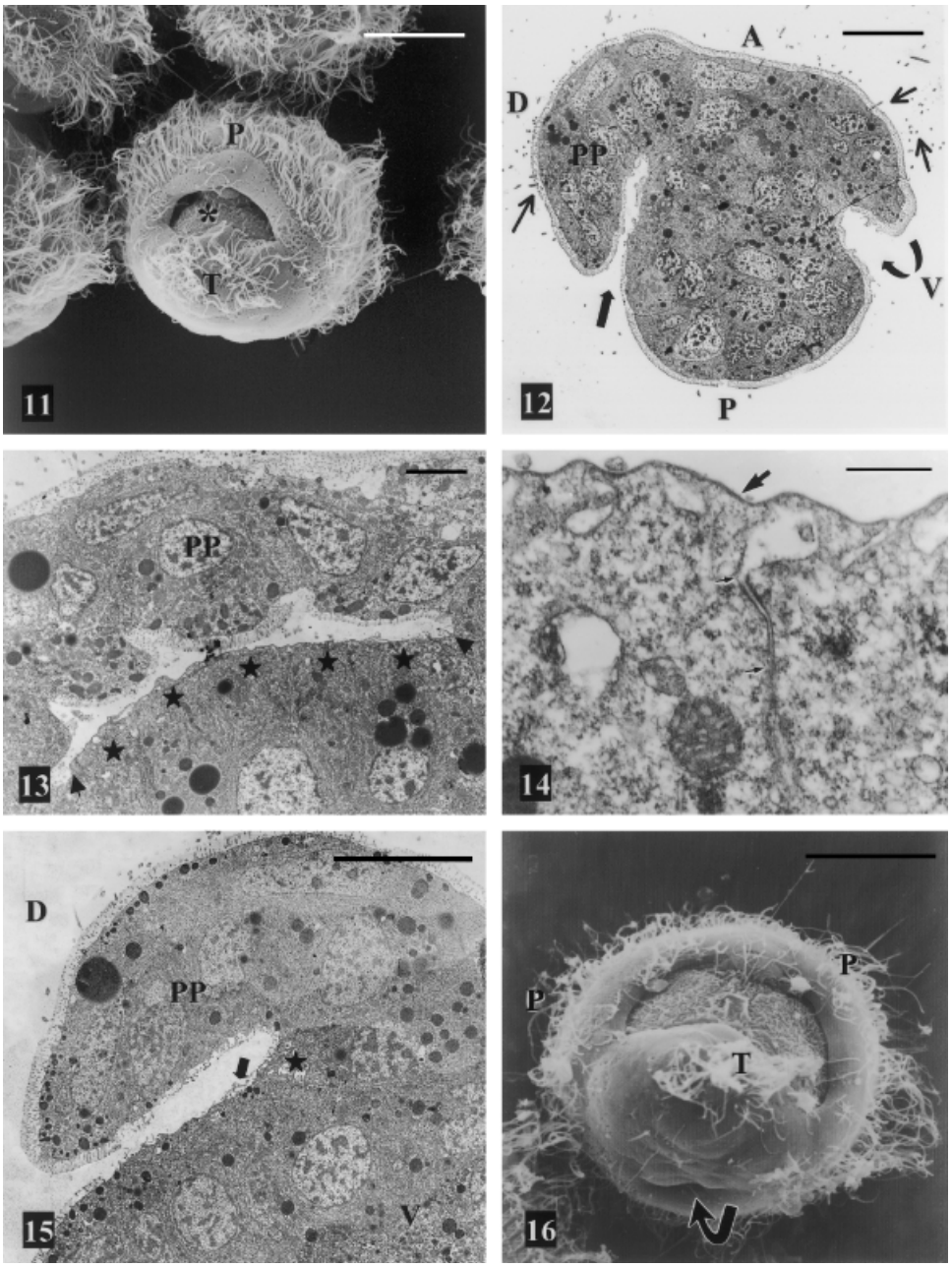

Figs. 11–16. Shell-field differentiation, at T_0+9 h, in gastrulae of *Chione cancellata*. **Fig. 11.** The trochophore larva is spherical and motile. The new shell material appears as a transverse pad (asterisk) with a wrinkled surface. It will progressively assume a dumbbell shape. P, prototroch; T, telotroch. Scanning electron microscopy (SEM). Scale bar, 10 μm. **Fig. 12.** Sagittal section. Similar to the stage observed 3 h earlier, this young trochophore has two cavities: the blastopore (curved arrow) with regular microvilli is located ventrally (V) whereas the open cave (straight arrow) is located dorsally (D). The floor of this cave is constituted by the shell field (delimited by arrowheads); small arrows indicate the cilia of the prototroch. The dorso-ventral axis (DV) extends through the prototrochal pad (PP) up to the blastopore. AP, antero-posterior axis. Transmission electron microscopy (TEM). Scale bar, 10 μm. **Fig. 13.** Cross-section through the prototrochal pad (PP) and shell field (delimited by arrowheads). At this stage, the apical poles of the shell-field cells (stars) are covered by a dense pellicle, which constitutes the periostracal material that appears wrinkled in **Fig. 11.** TEM. Scale bar, 10 μm. **Fig. 14.** High magnification of the periostracum, which appears as a dense line (arrow) covering the apical poles of two adjacent shell-field cells. The junction complex is delineated by small arrows. TEM. Scale bar, 0.5 μm. **Fig. 15.** Sagittal section of the open cave through the dorso-ventral axis (DV), showing the prototrochal cells (PP) and the shell-field cells which bear scarce microvilli at the far end of the cave (star). Next cells of the shell field are already covered by the new periostracum (arrow). TEM. Scale bar, 10 μm. **Fig. 16.** Saddle-stage trochophore at T_0+10 h. Bilateral symmetry is established, while the trochophore is still spherical. Curved arrow, blastopore; P, cilia from the prototroch; T, telotroch. SEM. Scale bar, 10 μm.

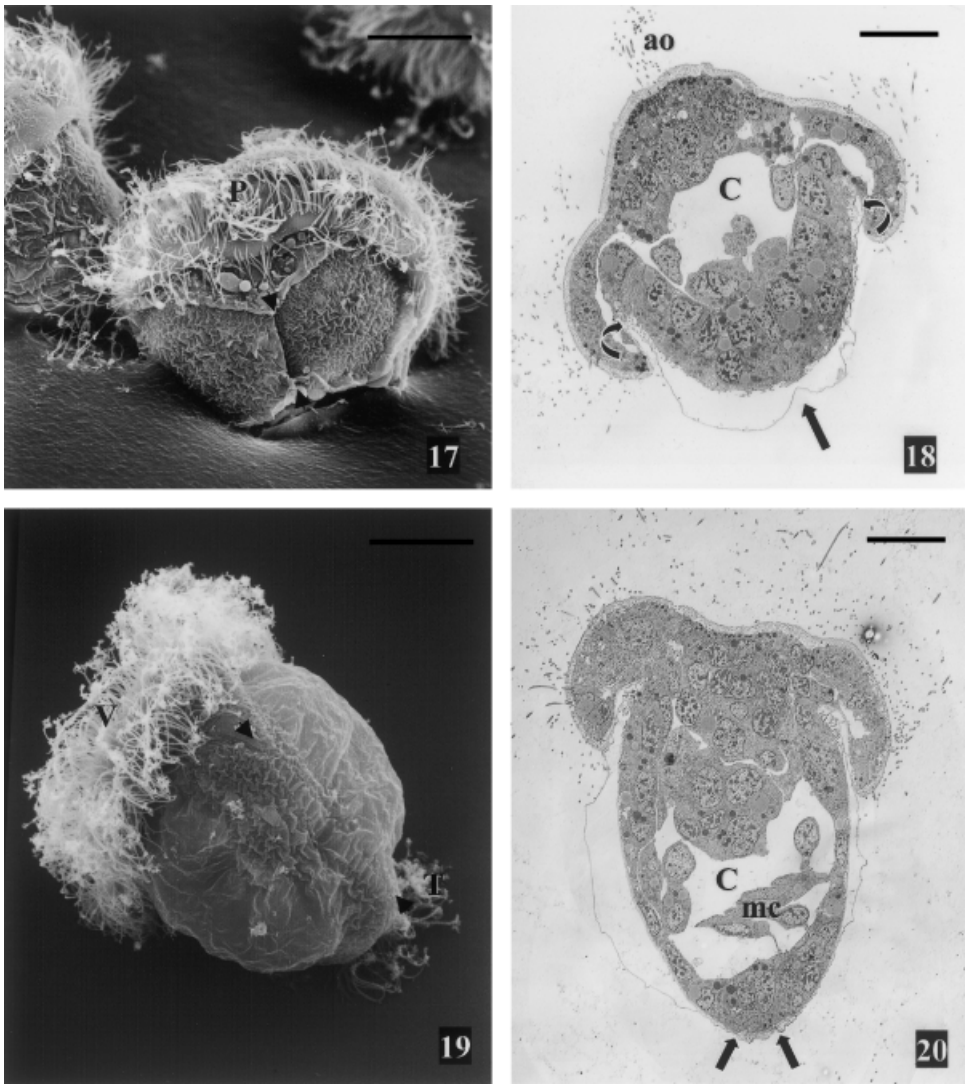

Figs. 17–20. Trochophores of *Chione cancellata* at T_0+12 h and T_0+15 h. Scale bars, 10 μm. **Fig. 17.** Postero-lateral view of a trochophore at T_0+12 h. The two lobes of the saddle-shaped shell field are expanding over the body. Bilateral symmetry is now obvious and the hinge line is well delineated (arrowheads). P, prototroch. Scanning electron microscopy (SEM). **Fig. 18.** Transverse section of a 12-h-old trochophore. Periostracum, as a fine line, appears attached both to the hinge (straight arrow) and to the mantle edge (curved arrows). It delineates the area in which the calcified layer of the shell will appear. Opposite to the hinge, the apical sense organ (ao) is located at the center of the prototroch, which will progressively develop into a velum. C, coelom. Transmission electron microscopy (TEM). **Fig. 19.** Trochophore at T_0+15 h. The valves, while covering the entire body and compressing the trochophore laterally, still appear uncalcified as suggested by their wrinkled aspect. The velum (V) is now well developed. The hinge is delineated by arrowheads. T, cilia from the telotroch. SEM. **Fig. 20.** Transverse section of a 15-h-old trochophore, showing insertion of the periostracum at the hinge area. The periostracum-secreting cells (arrows) are separated by non-secreting cells, which represent the inactive ligament secretory cells with microvilli at their apical pole. C, coelom; mc, muscle cells. TEM.

induce the formation of two weak depressions. The larger one featuring the shell field is located dorsally to the other, which is the blastopore. Thus, there are two independent structures with distinctive functions. The embryo already possesses a few cilia, located in the anterior region, which prefigure the future prototroch (Fig. 6).

At T_0+6 h, the dorsal region is marked by an open cave, which is expanding under and posterior to the developing prototrochal pad (Fig. 7). A TEM section of the embryo indicates that the floor of this open cave constitutes the shell field, and its roof is the lower face of the prototrochal pad (Fig. 8). The shell field, which is part of the ectodermal layer without

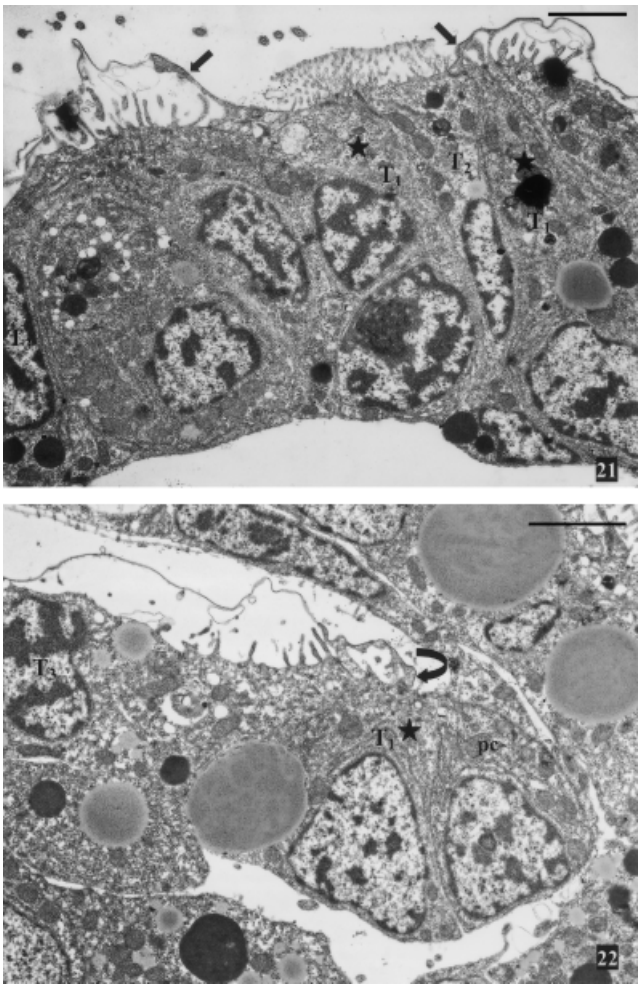

Figs. 21, 22. Details of periostracum insertion. Transmission electron microscopy (TEM). Scale bars, 0.5 μm. **Fig. 21.** The periostracum (arrows) originates at the hinge. It is produced by T1 secreting cells (stars) which are separated by non-secreting T2 cells characterized by numerous microvilli at their apical pole. The T1 secreting cells in contact with these inactive ligament secretory cells (T2) bear sparse and irregular microvilli covered by the dense pellicle of the periostracum. T3 cells, covered by the periostracum, are devoid of microvilli. **Fig. 22.** Origin of the periostracum (curved arrow) at the mantle margin emanating from secretory T1 cells (star). The secretory T1 cells in contact with the inner prototrochal cells (pc) are characterized by scarce microvilli that are covered by the dense pellicle of periostracum. T3 cells, covered by the periostracum, are devoid of microvilli.

any invagination process (Fig. 9), is characterized by scarce microvilli (Figs. 9, 10). The blastopore is located ventrally and, according to SEM views, it appears smaller than the open cave (Fig. 7). The developing archenteron is characterized by a brush border constituted by regular microvilli (Fig. 8).

At T_0+9 h, the late gastrula has differentiated into a typical motile trochophore (Figs. 11, 12) possessing a well-developed prototroch, composed of two ciliary crowns delimiting two regions: (i) the anterior pretrochal area bearing the long ciliary tuft of the apical sense organ and (ii) the posterior post-trochal area occupied by the blastopore in a ventral position and the shell field in a dorsal position. The latter is bordered on its posterior margin by the developing telotroch (Fig. 11). The lower face of the prototrochal pad still constitutes the roof covering the shell field (Fig. 12) as described for earlier embryos (Fig. 8). The cells located under the shell field are undifferentiated embryonic cells (Figs. 12, 13). At higher magnification, a dense pellicle is observed covering the apical pole of the shell-field cells (Figs. 13, 14), which appears wrinkled in SEM view (Fig. 11). The shell field and prototrochal pad remain in close contact (Figs. 15, 16).

At T_0+12 h, the shell material of the old trochophore spreads out and differentiates into two discrete lobes expanding over the body. Thus, the trochophore is laterally compressed (Figs. 17, 18). Moreover, the lobes (i) pull forward the ciliated crown of the prototroch emerging anteriorly to form the velum and (ii) pull downward the telotroch. Bilateral symmetry is now obvious and the hinge line is well delineated whereas the valves appear, as yet, not calcified (Fig. 17). The periostracum inserts both to the hinge and to the mantle edge (Fig. 18). It delineates the area in which the calcified layer of the shell will develop. At this stage of development, the apical sense organ appears to be comprised of a few ciliated cells with basal nuclei (Fig. 18).

From T_0+15 h to hatching, both uncalcified valves continue to expand and become thicker, compressing the trochophore laterally (Figs. 19, 20). The valves now completely enclose the soft body of the embryo (Fig. 20). At hinge, the periostracum emerges from secreting cells (T1) separated by non-secreting cells (T2) (Fig. 21). The numerous microvilli of the T2 cells are uncovered whereas the periostracum spreads from T1 cells over non-secreting cells (T3). T2 cells represent ligament secretory cells that are not yet active (Fig. 21). T1 secreting cells bear a few covered microvilli, whereas T3 cells are devoid of microvilli (Fig. 20). At the mantle margin, the periostracum inserts at similar T1 secreting cells (Fig. 22).

At T_0+23–24 h, the newly hatched veliger larva is enclosed in the calcified prodissoconch I (Fig. 23), characterized by its smooth surface (Fig. 24). In TEM views, a secondary layer is identified between the mantle tissue and the single layer of periostracum. The internal organization of this secondary layer is

not obvious at this stage (Fig. 25). The newly calcified shell layer, covered by periostracum, encloses the veliger larva from hinge to mantle edge. Straight-hinge veliger larvae of *C. cancellata* range 85–95 μm in shell length, with a hinge length of 55–60 μm.

At this stage, the functional velum is composed of four bands of cilia (Fig. 22): one inner pre-oral band, one outer pre-oral band, an adoral band, and the post-oral band surrounding the mouth. The outer pre-oral band is composed of the inner and outer rows of cirri, each cirrus being composed of 5–7 cilia stuck together (Figs. 26, 27). According to TEM, the kinetochores of these cilia are also linked to one another (Fig. 28). The innermost cells of the outer pre-oral band are adjacent to the mantle edge secreting cells. Therefore, the periostracal groove is located between the mantle cells and the velum cells. When the larval valves are closed, the ciliary bands of the velum fold into the pallial cavity overlying the apical organ and mouth (Figs. 23, 26).

The apical sense organ remains poorly developed. It appears to be composed of a few ciliated cells with

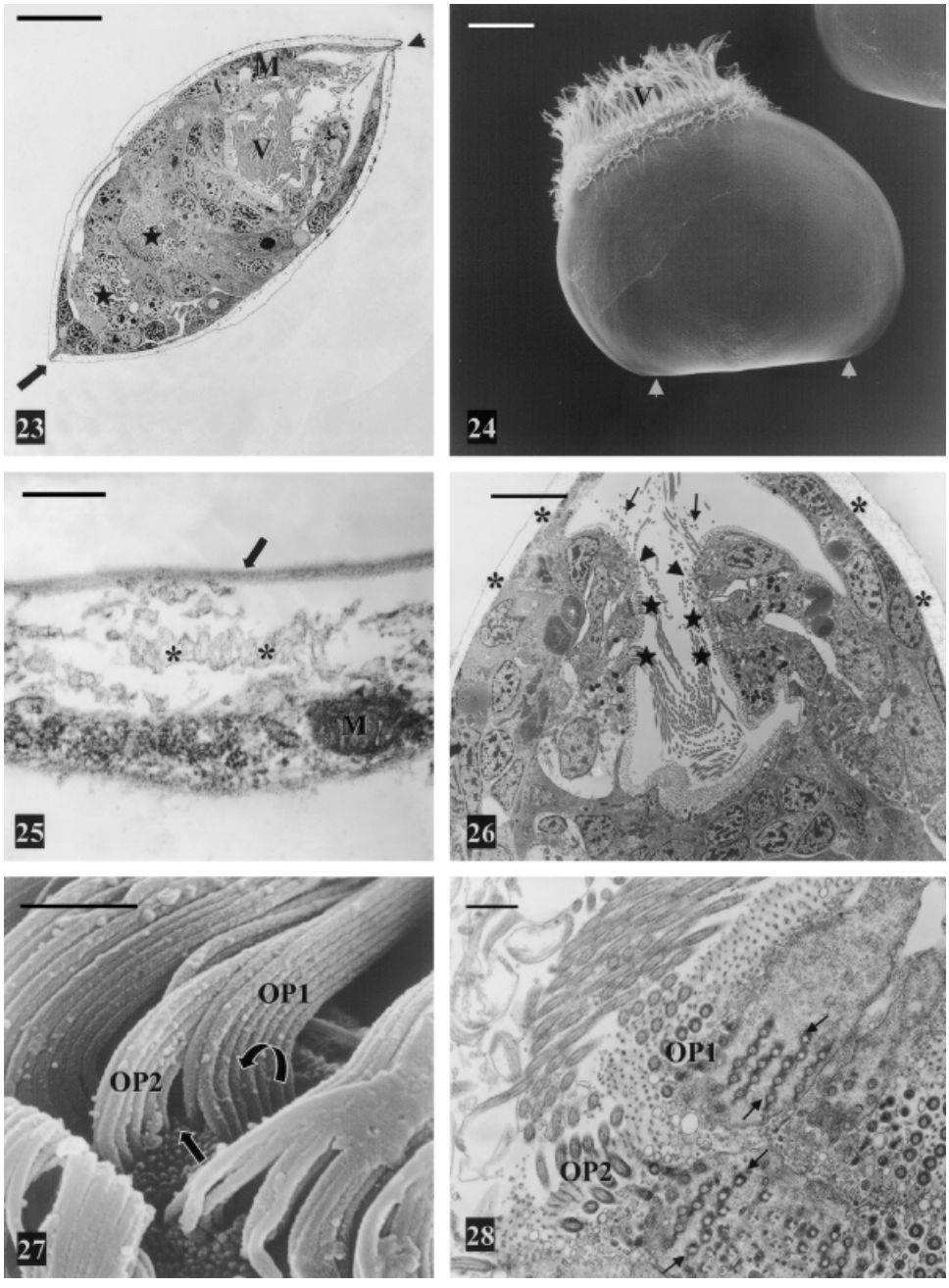

basal nuclei and numerous mitochondria (Fig. 29). Their normal cilia possess long double striated roots sinking into the cytoplasm up to the nucleus.

The digestive tract remains rudimentary. Its anterior part, from the mouth up to the stomach, is in close contact with the apical sense organ (Figs. 23, 29). The oesophagus appears non-ciliated at this stage (Fig. 29), whereas the stomach and the gut are heavily ciliated (Fig. 23).

Discussion

Embryonic development

Embryonic development in *Chione cancellata* is very similar to that of the venerid *Anomalocardia brasiliana* Gmelin 1791 (Mouëza et al. 1999). Oocytes have a small size and a limited vitelline supply typical of planktotrophic development (Ockelmann 1965). The average size of 60 μm described in this study is smaller than the average of 74 μm stated by D'Asaro (1967). The reasons for this difference of ~25% cannot be explained. D'Asaro (1967) described a small polar lobe after fertilization, which was never observed in our study. The embryonic stages of *C. cancellata* are fairly rapid and similar to those of *A. brasiliana,* with a ciliated blastula 3 h after fertilization, a typical trochophore 6 h later, and a fully developed veliger by 24 h at 25°C. It is difficult to compare age at various stages of development with those described by D'Asaro, because of mismatches between the description and the schedule of development.

During gastrulation, the cave in which the shell field will develop appears well before the formation of the prototroch. Authors do not agree on the order of appearance of these two structures (for review, see Waller 1981), but a sequential sampling at hourly intervals confirms that, at least in small tropical venerids, this cave appears when the gastrula possesses only a few cilia (Mouëza et al. 1999; this study).

The size of the D-stage larvae is not homogeneous for *C. cancellata*. D'Asaro (1967) described a veliger with a shell length of 100–125 μm, whereas LaBarbera & Chanley (1970) found a shell length of ~90 μm. In our experiments, 24-h D-stage larvae were ~90 μm long, with a straight hinge of 60 μm on average. These variations in size for the first stage of larval development are difficult to reconcile.

Shell differentiation

Other authors working on shell differentiation during the embryonic development of bivalve molluscs have reported the invagination process described one century ago by Stepanoff (in Kniprath 1980). It has been suggested that the invagination needs to close either completely before the shell formation, as in the case of *Mytilus galloprovincialis* (Kniprath 1980) and *Pecten maximus* (Casse et al. 1998), or partially, as proposed for *Spisula solidissima* (Eyster & Morse 1984). These studies related to bivalves were based on a process described from gastropods (Kniprath 1980; Eyster 1983). Gastropods are univalve, whereas in bivalves, the shell is composed of two discrete valves articulating at a hinge and linked by a ligament which can be located inside or outside the shell. None of the previous studies shows how these different parts of the bivalve shell are built. Observations at the ultrastructural level during embryonic development of *C. cancellata* lead us to propose an alternate interpretation of shell differentiation including hinge differentiation, which appears at the trochophore stage as an independent phenomenon.

←

Figs. 23–28. D-stage veliger larvae of *Chione cancellata*. **Fig. 23.** At T_0+24 h, the veliger larva is enclosed in the calcified prodissoconch I from the hinge (arrow) to the mantle edge (arrowhead). The new calcified shell, which appears white, is covered by the periostracum. M, mantle; stars, sections of the digestive tract; V, cilia from the velum. Transmission electron microscopy (TEM). Scale bar, 1 μm. **Fig. 24.** Early veliger or D-larva at T_0+24 h, enclosed within the prodissoconch I. The velum (V) extends between the shell valves during swimming or feeding. The straight hinge is indicated by arrowheads. Scanning electron microscopy (SEM). Scale bar, 1 μm. **Fig. 25.** Cross-section of the prodissoconch I of a veliger larva. A secondary layer, located between the mantle (M) and the periostracum (arrow), encloses the first calcium crystals (asterisks) of the shell. TEM. Scale bar, 0.5 μm. **Fig. 26.** Apical section of a veliger larva. The rows of velar cilia are withdrawn inside the valves. Cilia from the post-oral (small arrows) and adoral (arrowheads) bands are randomly distributed. The outer pre-oral band is composed of a double row in which cilia appear to be linked (stars). Asterisks: prodissoconch I shell. TEM. Scale bar, 10 μm. **Fig. 27.** View of ciliary bands of the velum. The outer pre-oral band of the velum consists of double cirri (OP1 and OP2) with up to 7 cilia per row (curved arrow). The inner cirrus (OP1) is separated from the outer cirrus (OP2) by a narrow space (arrow). SEM. Scale bar, 1 μm. **Fig. 28.** Section through the velar margin showing the insertion of the pre-oral cirri. Confirming the SEM view, the outer pre-oral band bears two bands of cirri (OP1 and OP2) with compound cilia. Each band is composed of parallel ranks of cirri, each cirrus including 5–7 cilia in a row, the kinetochores of which (small arrows) are linked to one another. TEM. Scale bar, 1 μm.

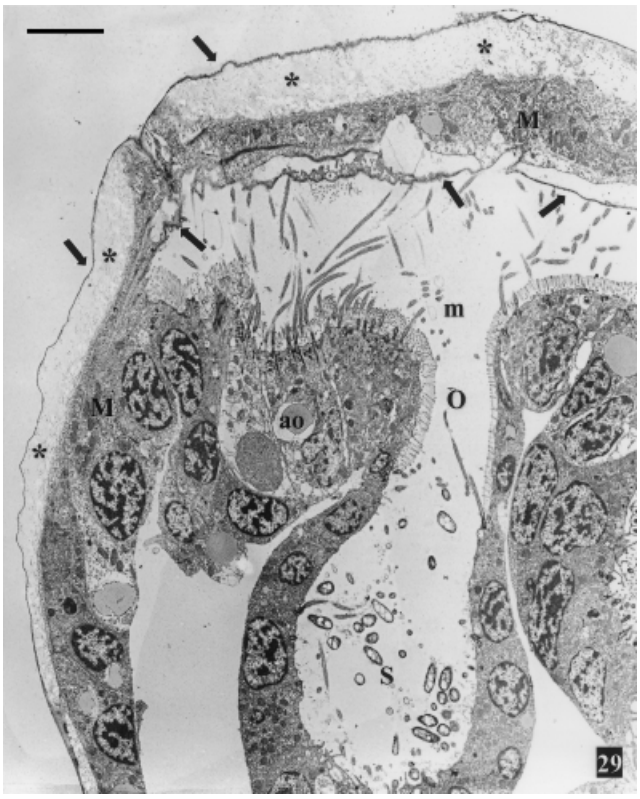

Fig. 29. Transmission electron microscopy section showing the velar margin, the apical sense organ, and the anterior part of the digestive tract. The apical sense organ (ao) is composed of a few cells with basal nuclei and cilia characterized by long double-ciliary roots up to the nucleus. The sagittal section of the digestive tract gets through the mouth (m), the oesophagus (O), which seems to lack cilia at this stage, and the stomach (S). The lumen of the stomach contains numerous bacteria ingested by the veliger. The periostracum (arrows) delineates the unique mantle fold. Asterisks, prodissoconch I shell; M, mantle. Scale bar, 5 μm.

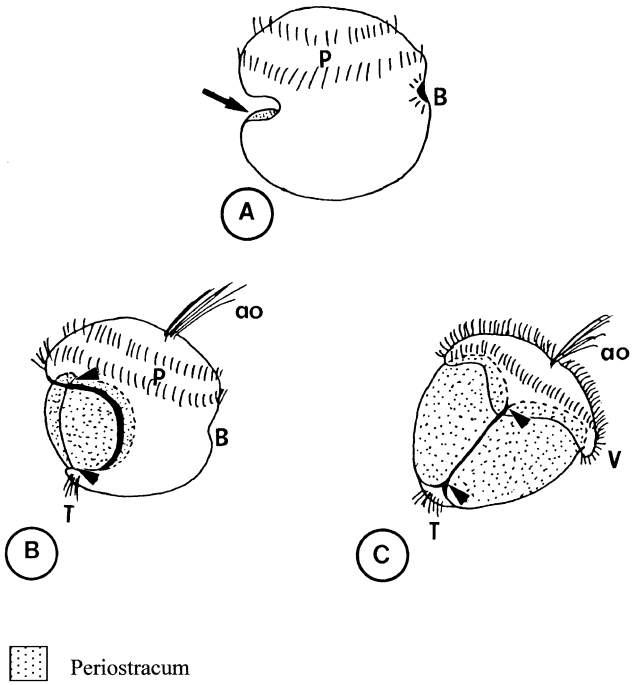

Fig. 30. Shell-field differentiation in *Chione cancellata:* gastrula to trochophore transition. **A.** Dorso-lateral view of a young gastrula, 6 h after fertilization. The dorsal region of this almost spherical embryo is identified by the shell field (arrow), which is expanding below the prototroch and constituting the floor of the open cave. **B.** Dorso-lateral view of a trochophore, 12 h after fertilization, which is still nearly spherical. The extension of the shell field by epiboly has already begun. The new shell material expands gradually over the body, covering both sides of the embryo between the prototroch and the telotroch. The uncalcified valves are separated by the hinge line (arrowheads). **C.** Dorsal view of a late trochophore, 15 h after fertilization. Both uncalcified valves continue to expand, compressing the trochophore laterally. Thus, the prototroch is displaced ventrally and constitutes the velum. The valves enclose now almost completely the soft body of the embryo. The hinge is indicated by arrowheads. ao, apical organ; B, blastopore; P, prototroch; T, telotroch; V, velum.

A comparative TEM and SEM analysis shows that morphogenetic movements put the shell field in a dorsal position below the future prototroch (Fig. 30), which develops a pad of ciliated cells overhanging the shell field. The shell field, which includes both shell and ligament secretory cells, does not migrate inward and never builds an invagination by itself. The prototrochal pad and the shell field constitute an open cave, at the far end of which they are in close contact.

The periostracum is the first observable part of the shell. It is elaborated by T1 cells, which may be assimilated to stem cells described for the proliferation of various epithelial cells. At first step, the periostracum appears continuous because the apical poles of the ligament secretory T2 cells are covered by the adjacent T1 cells (Fig. 31). When the T2 cells reach the surface of the shell-field epithelium, they set apart the T1 cells, and the hinge line becomes obvious (Fig. 31). Thus, the intrusion of the T2 cells between T1 cells is the event at the origin of the typical bivalve shell before building up the ligament.

T3 cells, issued from T1 stem cells, do not elaborate periostracum material; they produce the second organic layer of the shell and are involved in the calcification of the shell. At this stage, the three types of shell secretory cells are differentiated. The first type (T1 cells) elaborates the first organic layer of

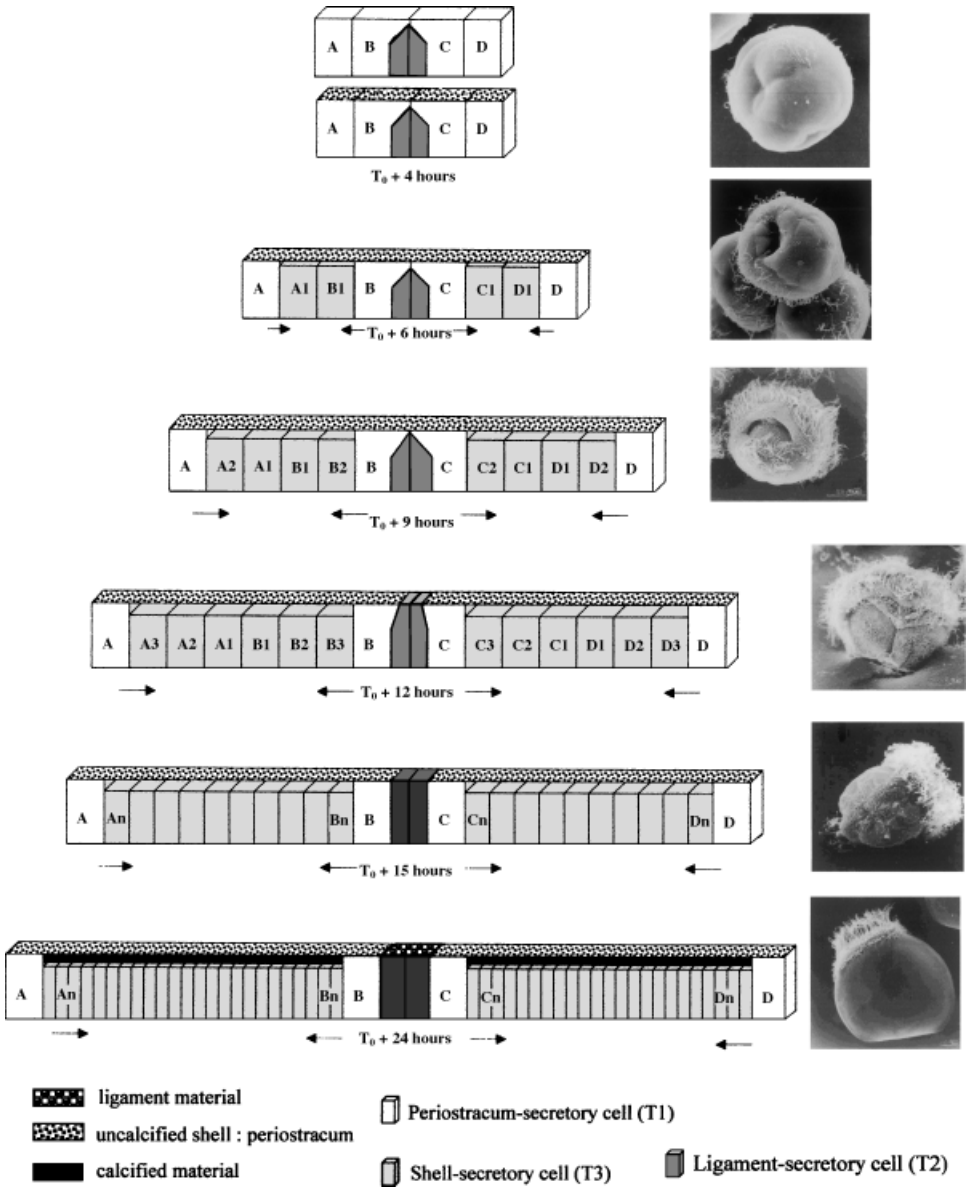

Fig. 31. Shell-field and hinge differentiation in *Chione cancellata* during embryonic development from early gastrula to D-stage veliger. The figure presents pairwise comparisons between scanning electron microscope views and diagrammatic cross-sections through the shell field at successive stages of development. T_0+4 h: The shell field includes both shell and ligament secretory cells. The apical pole of the ligament secretory T2 cells is covered by the periostracum-secreting T1 cells. From T_0+6 h, the proliferation of the periostracum-secreting T1 cells is similar to the process described for epithelial stem cells. The new T3 cells do not elaborate periostracum material. Up to T_0+12 h, the expansion of the shell field is only due to the proliferation of the daughter T3 cells. From T_0+12 h, the ligament secretory T2 cells reach the surface of the shell-field epithelium, set apart the T1 cells, and create the two valves of the bivalve shell. The hinge field becomes obvious. At T_0+24 h, T3 cells elaborate a secondary organic layer which encloses calcium crystals. Therefore the valves, which are now calcified, lose their wrinkled aspect. T2 cells are now secreting the ligament material.

the shell (i.e., the periostracum). The second type (T2 cells) elaborates a material specific to the ligament. The third type (T3 cells) builds up the secondary organic layer that will enclose calcium crystals. Each shell valve comprises two sets of T1 stem cells, one at the hinge and the other at the mantle edge, separated by an increasing number of daughter T3 cells.

The new shell material spreads out, pushing the adjacent tissues as growth proceeds (Fig. 30), over-

lapping the embryo, pushing aside the prototrochal pad to the top and to the front, and the telotroch to the bottom and to the front of the trochophore. Mantle epiboly and shell expansion play a major role in the transformation from trochophore to veliger, by compressing the soft body and displacing the prototroch that becomes the velum (Fig. 30).

Thiele (in Kniprath 1980) disclaimed, as early as a century ago, the relationship between bivalve and gastropod shell-field development; he considered that the two types of shell were only analogous. However, his proposal that the formation of the pallial isthmus structures preceded that of the valves had not been investigated; the present article demonstrates that the shell valve partition precedes ligament formation.

Further investigations will be necessary to understand (i) when and how the T1 cells adjacent to the T2 cells stop to elaborate the periostracum, so that its expansion will be only due to the T1 cells of the mantle edge and (ii) when and how T2 cells begin to elaborate the ligament.

Velum and mantle

In this study, we confirm that the two outer preoral bands consist of two long cirri composed of 5–7 cilia separated by a narrow space, as described in *A. brasiliana* for 3-day-old veligers (Mouëza et al. 1999). The TEM views of this organ confirm the low number of cilia involved in the velum, unlike other species (for review, see Cragg 1996). Kinetosomes are linked to each other in rows, suggesting that the cilia constituting internal and external cirri of the outer preoral band move together at the same time. Such movements could be involved in transferring food particles to the mouth, as for the adoral band. However, it is difficult to confirm that the velum of 24-h-old veligers of *C. cancellata* possesses an inner preoral band, as described in 3-day-old veligers of *A. brasiliana* (Mouëza et al. 1999). All other bands constituting the velum are similarly organized. The cells that secrete the periostracum are still directly in contact with the most-internal cells of the velum, which will soon disappear. Velar involution during the pediveliger stage is not well understood and needs further investigation. Before velar involution, the mantle edge comprises only one fold, representing the outer fold (Yonge 1957). Further investigations will be necessary to understand how and when the inner and middle folds, typical of the adult structure of the mantle edge, differentiate.

Acknowledgments. We gratefully acknowledge John Zardus' very helpful comments as reviewer of the manuscript. This work was carried out at SIMAG (Service Interrégional de Microscopies des Antilles et de la Guyane).

References

Abbott RT 1974. American Seashells. Van Nostrand Reinhold, New York. 663 pp.

Bellolio G, Lohrmann K, & Dupré R 1993. Larval morphology of the scallop *Argopecten purpuratus* as revealed by scanning electron microscopy. Veliger 36: 332–342.

Carriker MR & Palmer RE 1979. Ultrastructural morphogenesis of prodissoconch and early dissoconch valves of the oyster *Crassostrea virginica*. Proc. Natl. Shellfish Assoc. 69: 103–128.

Casse N, Devauchelle N, & Le Pennec M 1998. Embryonic shell formation in the scallop *Pecten maximus* (Linnaeus). Veliger 41: 133–141.

Cragg SM 1996. The phylogenetic significance of some anatomical features of bivalve veliger larvae. In: Origin and Evolutionary Radiation of the Mollusca. Taylor J, ed., pp. 326–371. Oxford University Press, Oxford.

D'Asaro CN 1967. The morphology of larval and post-larval *Chione cancellata* Linné (Eulamellibranchia Veneridae) reared in the laboratory. Bull. Mar. Sci. 17: 949–972.

Eyster LS 1983. Ultrastructure of early embryonic shell formation in the opistobranch gastropod *Aeolidia papillosa*. Biol. Bull. 165: 394–408.

Eyster LS & Morse MP 1984. Early shell formation during molluscan embryogenesis with new studies on the surf clam *Spisula solidissima*. Am. Zool. 24: 871–882.

Frenkiel L & Mouëza M 1979. Développement larvaire de deux Tellinacea, *Scrobicularia plana* (Semelidae) et *Donax vittatus* (Donacidae). Mar. Biol. 55: 187–195.

Glauert AM 1975. Practical Methods in Electron Microscopy. 3 (1): Fixation, Dehydration and Embedding of Biological Specimens. Elsevier, Amsterdam. 208 pp.

Gros O, Frenkiel L, & Mouëza M 1997. Embryonic, larval, and post-larval development in the symbiotic clam, *Codakia orbicularis* (Bivalvia: Lucinidae). Invertbr. Biol. 116: 86–101.

Gros O, Duplessis MR, & Felbeck H 1999. Embryonic development and endosymbiont transmission mode in the symbiotic clam *Lucinoma aequizonata* (Bivalvia: Lucinidae). Invertbr. Reprod. Dev. 36: 93–103.

Hodgson CA & Burke RD 1988. Development and larval morphology of the spiny scallop *Chlamys hastata*. Biol. Bull. 174: 303–318.

Humphreys W 1969. Initial shell formation in the bivalve *Mytilus edulis*. Proc. Electron. Microsc. Soc. Am. 27: 272–273.

Kniprath E 1980. Larval development of the shell and the shell gland in *Mytilus* (Bivalvia). Wilhelm Roux's Arch. Dev. Biol. 188: 201–204.

Labarbera M & Chanley PE 1970. Larval development of *Chione cancellata* L. (Veneridae, Bivalvia). Chesapeake Sci. 11: 42–49.

Loosanoff V & Davis HC 1963. Rearing of bivalve larvae. Adv. Mar. Biol. 1: 1–136.

Loosanoff V, Davis HC, & Chanley PE 1966. Dimensions and shapes of larvae of some marine bivalve mollusks. Malacologia 4: 351–435.

Mouëza M, Gros O, & Frenkiel L 1999. Embryonic, larval, and postlarval development of the tropical clam *Anomalocardia brasiliana* (Mollusca: Bivalvia, Veneridae). J. Moll. Stud 65: 73–88.

Ockelmann KW 1965. Developmental types in marine bivalves and their distribution along the Atlantic coast of Europe. In: Proceedings of the First European Malacology Congress 1962. Cox LR & Peake JF, eds., pp. 25–35. Conch. Soc. G.B. and Ireland and Malac. Soc. London, London.

Rios EC 1985. Seashells of Brasil. Empressas Ipiranga, Rio Grande RS XII, Brazil.

Sastry AN 1979. Pelecypoda (excluding Ostreidae). In: Reproduction of Marine Invertebrates, Vol. 5. Molluscs. Pelecypods and Lesser Classes. Giese AC & Pearse JS, eds., pp. 113–292. Academic Press, New York.

Stephenson RL & Chanley PE 1979. Larval development of the cockle *Chione stutchburyi* (Bivalvia: Veneridae) reared in laboratory. New Zeal. J. Zool. 6: 553–560.

Waller TR 1981. Functional morphology and development of veliger larvae of the European oyster *Ostrea edulis* Linné. Smithsonian Contr. Zool. 328: 1–70.

Warmke GL & Abbott RT 1962. Caribbean Seashells. Livingston Narberth, Narbeth, PA. 348 pp.

Yonge CM 1957. Mantle fusion in Lamellibranchia. Pubbl. Staz. Zool. Napoli 29: 151–171.

Zardus JD & Morse MP 1998. Embryogenesis, morphology and ultrastructure of the pericalymma larva of *Acila castrensis* (Bivalvia: Protobranchia: Nuculoida). Invertbr. Biol. 117: 245–252.